Robust Seed Template Generation for Interactive Image Segmentation

Mario Amrehn[1], Stefan Steidl[1], Markus Kowarschik[2], Andreas Maier[1,3]

[1]Pattern Recognition Lab., Friedrich-Alexander-Universität Erlangen-Nürnberg (FAU), Germany
[2]Siemens Healthcare GmbH, Erlangen, Germany
[3]Erlangen Graduate School in Advanced Optical Technologies (SAOT), Germany

FRIEDRICH-ALEXANDER UNIVERSITÄT ERLANGEN-NÜRNBERG
FACULTY OF ENGINEERING

SIEMENS Healthineers

Introduction

Basic Situation

In interactive medical image segmentation, anatomical structures are extracted.

Usability studies [1], [2] illustrate, that users spend significant amounts of time and effort in the beginning of an interactive workflow to achieve segmentation accuracies also reachable by fully automated systems [3].

Challenges

Only after this time consuming first phase, the efficient selective refinement of current segmentation results begins.

Automated initial seeding approaches may place erroneously labeled seeds challenging to detect and replace for a human, thus substantially impact the overall segmentation quality.

Our Approach

We propose an automatic seeding pipeline as well as a configuration based on saliency recognition, in order to skip the time-consuming initial interaction phase during segmentation.

A median Dice score of 68.22 % is reached before the first user interaction on the test data set with an error rate in seeding of only 0.088 %.

Data

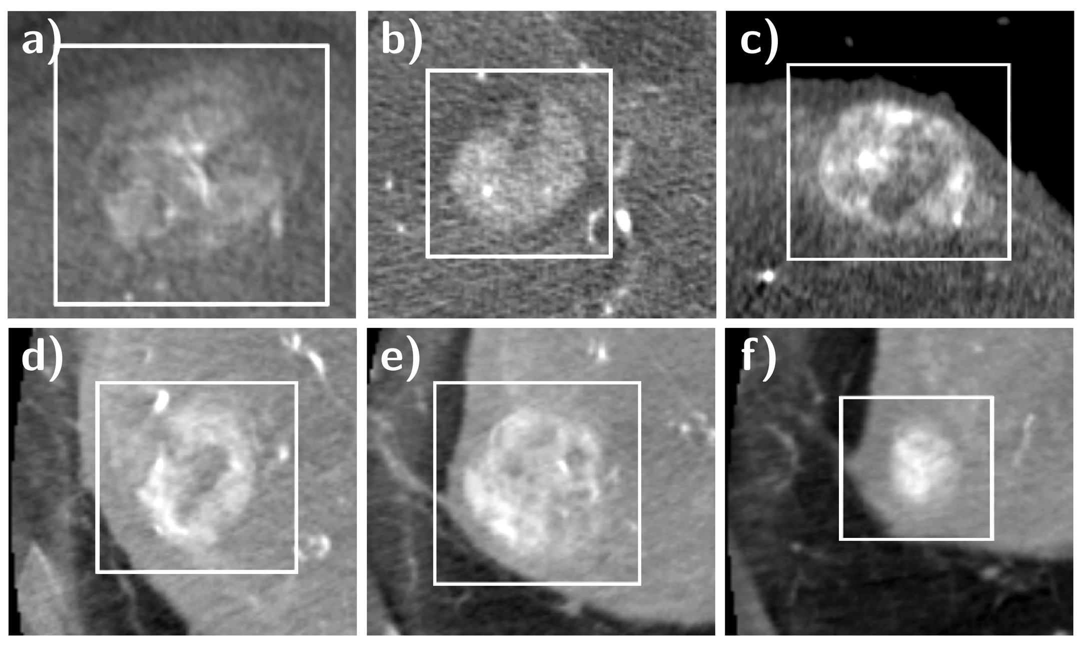

Challenges of hepatic lesion segmentation are (a) high diversity in gray-values, no typical shape, (b) intensity overlaps, (c) necrotic regions/patches, and (d–f) varying appearance of the same tumor between 2-D slices.

38 volumetric lesion images fully annotated by medical experts are used as GT segmentations.

Methods

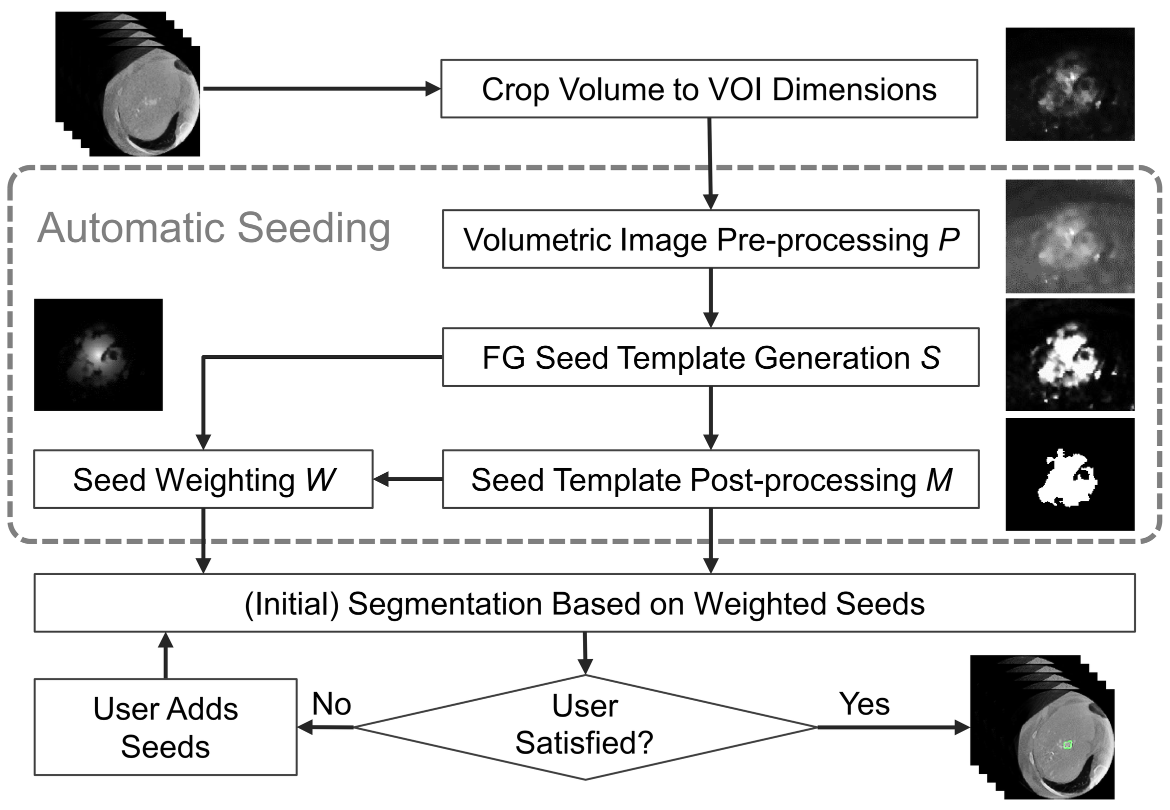

Interactive segmentation workflow. The dashed box indicates the automated seeding process defined by $(\mathbf{P}, \mathbf{S}, \mathbf{W}, \mathbf{M})$. Morphological operation $\mathbf{M}_{\{e,o\}}$ is binary erosion or opening, respectively.

[4] [5] [6] [7]

Saliency techniques originally designed for object detection in photographic images.

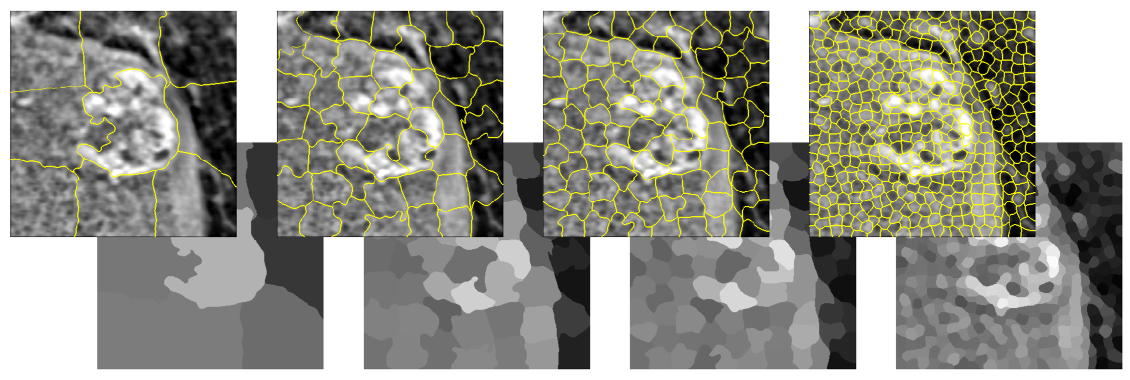

For saliency, SLIC [8] superpixels are used internally. Displayed are $\{0.1, 0.5, 1, 5\}$ % of pixels.

Otsu thresholding is used to binarize largest saliency scores. A Gaussian kernel is shifted to the center of mass for seeds' proximity weighting $\mathbf{W}$.

Results & Discussion

Quantitative Results

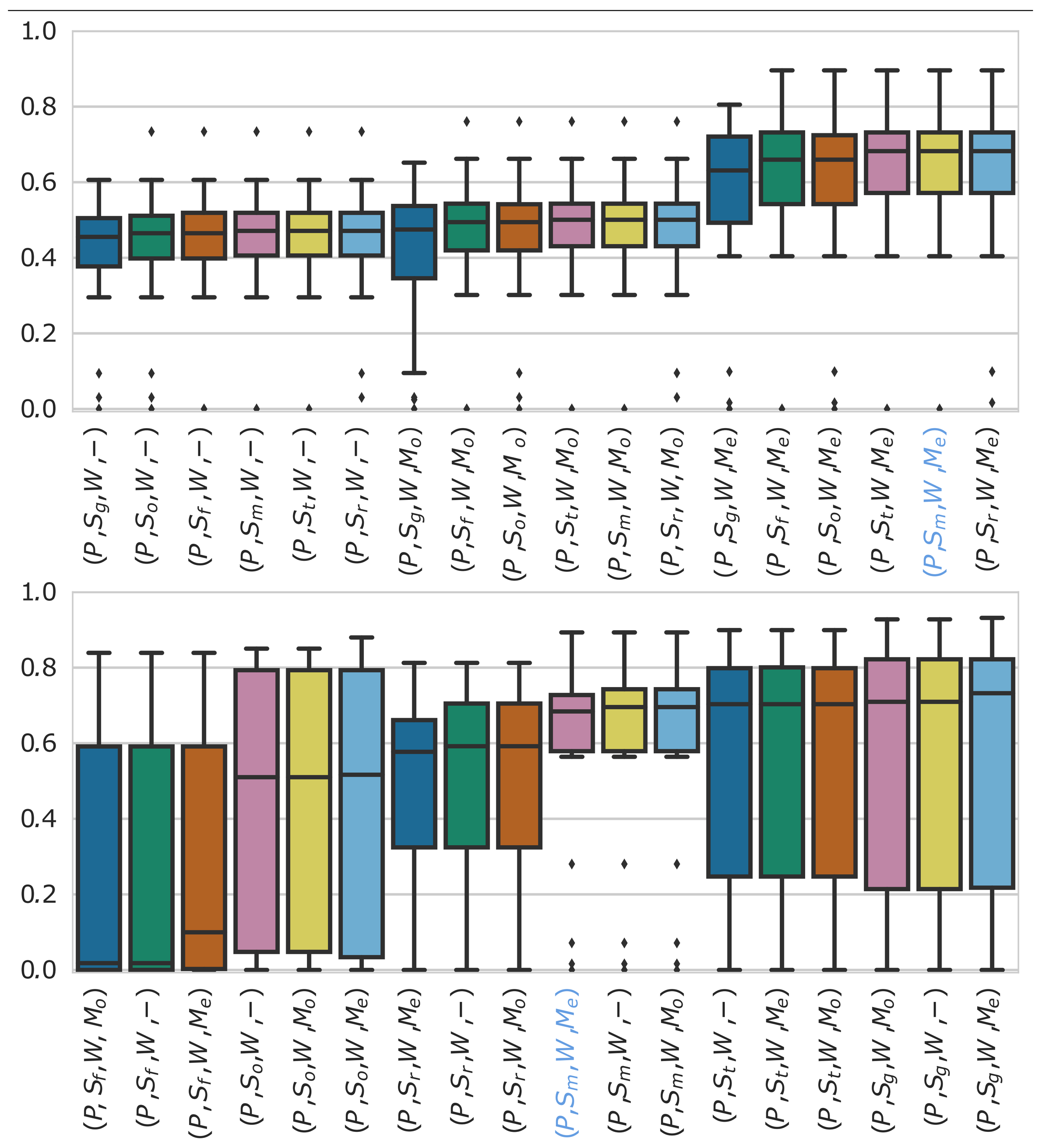

Evaluation of GC [9] (upper row) and RW [10] (lower row) segmentations' Dice scores. Proposed method $(\mathbf{P}, \mathbf{S}_m, \mathbf{W}, \mathbf{M}_e)$ is highlighted.

Qualitative Results

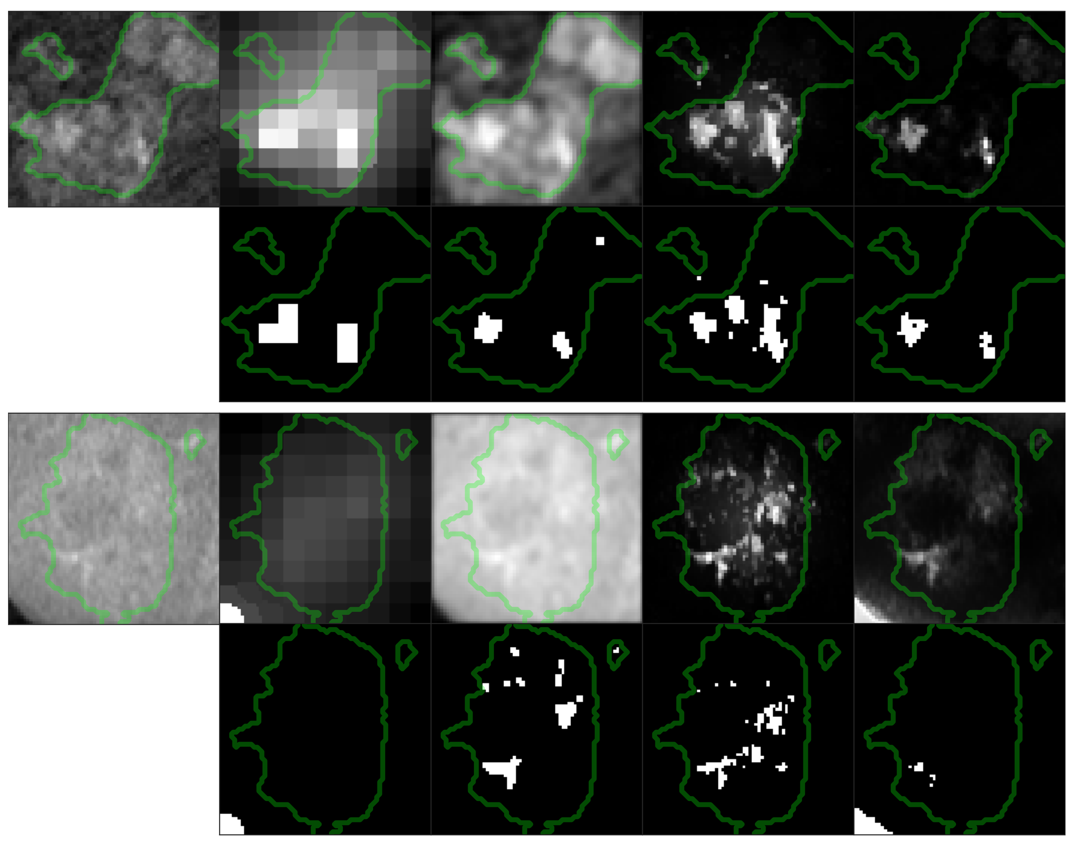

$\mathbf{S}_r$ [4] $\mathbf{S}_t$ [5] $\mathbf{S}_m$ [6] $\mathbf{S}_f$ [7]

Saliency maps (upper rows) from input image (leftmost column) utilizing different detection techniques $\mathbf{S}_{\{r,t,m,f\}}$. Seed masks (lower rows) are obtained via thresholding and weighting.

Annotated contour line depicted in green.

Method $(\mathbf{P}, \mathbf{S}_m, \mathbf{W}, \mathbf{M}_e)$ achieves the highest median Dice score for GC segmentation.

Conclusion

An automated seeding pipeline was defined and evaluated, which supports various saliency detection and thresholding based methods.

An extensive comparison of pipeline element selections resulted in the proposition of configuration $(\mathbf{P}, \mathbf{S}_m$ [6], $\mathbf{W}, \mathbf{M}_e)$ for pipeline usage.

$(\mathbf{P}, \mathbf{S}_m, \mathbf{W}, \mathbf{M}_e)$ yields high quality segmentation results as well as low FPR errors, crucial for successful automated seed placement.

Contact

✉ mario.amrehn@fau.de
☞ www5.cs.fau.de/~amrehn

References

[1] S. D. Jain *et al.*, "Predicting sufficient annotation strength for interactive foreground segmentation," in *ICCV*, 2013, pp. 1313–1320.
[2] F. Andrade *et al.*, "Supervised evaluation of seed-based interactive image segmentation algorithms," in *STSIVA*, 2015, pp. 1–7.
[3] A. Militzer *et al.*, "Automatic detection and segmentation of focal liver lesions in contrast enhanced ct images," in *ICPR*, 2010, pp. 2524–2527.
[4] W. Zhu *et al.*, "Saliency optimization from robust background detection," in *CVPR*, 2014, pp. 2814–2821.
[5] R. Achanta *et al.*, "Frequency-tuned salient region detection," in *CVPR*, 2009, pp. 1597–1604.
[6] J. Zhang *et al.*, "Minimum barrier salient object detection at 80 fps," in *ICCV*, 2015, pp. 1404–1412.
[7] F. Perazzi *et al.*, "Saliency filters: Contrast based filtering for salient region detection," in *CVPR*, 2012, pp. 733–740.
[8] R. Achanta *et al.*, "SLIC superpixels compared to state-of-the-art superpixel methods," in *TPAMI*, 2012, pp. 2274–2282.
[9] V. Vezhnevets *et al.*, "GrowCut: Interactive multi-label nd image segmentation by cellular automata," in *Graphicon*, 2005, pp. 150–156.
[10] L. Grady, "Random walks for image segmentation," in *TPAMI*, 2006, pp. 1768–1783.

Acknowledgment: The authors gratefully acknowledge the support of Siemens Healthcare GmbH, Forchheim, Germany. Concepts and information presented in this paper are based on research and are not commercially available.